

# High temperature QCD with three flavors of improved staggered quarks \*

C. Bernard <sup>a</sup>, T. Burch <sup>b</sup>, C.E. DeTar <sup>c</sup>, Steven Gottlieb <sup>d</sup>, Eric Gregory <sup>b</sup>, U.M. Heller <sup>e</sup>, J. Osborn <sup>c</sup>, R.L. Sugar <sup>f</sup>, and D. Toussaint <sup>b</sup>

<sup>a</sup>Department of Physics, Washington University, St. Louis, MO 63130, USA

<sup>b</sup>Department of Physics, University of Arizona, Tucson, AZ 85721, USA

<sup>c</sup>Physics Department, University of Utah, Salt Lake City, UT 84112, USA

<sup>d</sup>Department of Physics, Indiana University, Bloomington, IN 47405, USA

<sup>e</sup>CSIT, Florida State University, Tallahassee, FL 32306-4120, USA

<sup>f</sup>Department of Physics, University of California, Santa Barbara, CA 93106, USA

We present an update of our study of high temperature QCD with three flavors of quarks, using a Symanzik improved gauge action and the Asqtad staggered quark action. Simulations are being carried out on lattices with  $N_t = 4, 6$  and  $8$  for the case of three degenerate quarks with masses less than or equal to the strange quark mass,  $m_s$ , and on lattices with  $N_t = 6$  and  $8$  for degenerate up and down quarks with masses in the range  $0.2m_s \leq m_{u,d} \leq 0.6m_s$ , and the strange quark fixed near its physical value. We also report on first computations of quark number susceptibilities with the Asqtad action. These susceptibilities are of interest because they can be related to event-by-event fluctuations in heavy ion collision experiments. Use of the improved quark action leads to a substantial reduction in lattice artifacts. This can be seen already for free fermions and carries over into our results for QCD.

We are studying high temperature QCD with three flavors of improved staggered quarks [1] using a one-loop Symanzik improved gauge action and the Asqtad quark action [2,3]. Both the gauge and quark actions have all lattice artifacts removed through order  $a^2$  ( $a$  is the lattice spacing) at tree level, and are tadpole improved. Thus, the leading order finite lattice spacing artifacts are of order  $\alpha_s a^2, a^4$ . We consider two cases: 1) all three quarks have the same mass  $m_q$ ; and 2) the two lightest mass quarks have equal mass  $m_{u,d}$  and the mass of the third quark is fixed at that of the strange quark  $m_s$ . We refer to these cases as  $N_f = 3$  and  $N_f = 2 + 1$ , respectively.

Because it contains the Naik term [4] the Asqtad action has a significantly better dispersion relation for the quarks than the standard Kogut-Susskind and Wilson quark actions, which helps decrease lattice artifacts in the energy and pressure [1], and, as we shall see, for the quark number

susceptibilities. The Asqtad action also exhibits excellent scaling properties [5], and significantly better flavor symmetry properties than the conventional Kogut-Susskind action [2,6]. We estimate that for lattices with eight to ten time slices, the kaon will be heavier than the heaviest non-Goldstone pion in the neighborhood of the finite temperature transition or crossover.

We have attempted to vary the temperature while keeping all other physical quantities constant. To this end we have performed a set of spectrum calculations at  $a = 0.13$  fm and  $0.20$  fm for three equal mass quarks. Here, and throughout this work, we determine the lattice spacing from the static  $\bar{Q}Q$  potential, and express dimensionful quantities in terms of  $r_1$  defined by  $r_1^2 F_{\bar{Q}Q}(r_1) = 1$ , which leads to  $r_1 \approx 0.34$  fm. We determine  $m_s$  from the requirement that  $m_{\eta_{ss}}/m_\phi \approx 0.673$ . We have performed spectrum calculations at both lattice spacings with  $m_q = m_s, 0.6 m_s$  and  $0.4 m_s$ , with an additional

---

\*Presented by U.M. Heller and R.L. Sugar.

calculation at  $0.2 m_s$  in progress. We would like to carry out our thermodynamics studies with three equal mass quarks for  $m_{\eta_{ss}}/m_\phi$  fixed, but this quantity will, of course, vary slightly with lattice spacing if we keep  $m_q/m_s$  fixed. So, at  $a = 0.2$  fm we perform linear interpolations of  $m_{\eta_{ss}}^2$  and  $m_\phi$  in the quark mass to determine the precise values of  $m_q$  for which  $m_{\eta_{ss}}/m_\phi$  takes on the values found at  $a = 0.13$  fm. Then to determine the values of  $am_q$  and  $a$  for thermodynamics studies with  $0.13 \text{ fm} < a < 0.20 \text{ fm}$ , we perform linear interpolations of the logarithms of these quantities in the gauge coupling  $10/g^2$ .

Our approach for thermodynamics studies with  $m_{u,d} < m_s$  is quite similar. In this case we wish to vary the temperature keeping both  $m_\pi/m_\rho$  and  $m_{\eta_{ss}}/m_\phi$  fixed. We have therefore performed a set of spectrum calculations at  $a = 0.13$  fm and  $0.20$  fm with the mass of the light quarks,  $m_{u,d} = 0.6 m_s$ ,  $0.4 m_s$  and  $0.2 m_s$ . An additional spectrum calculation with  $m_{u,d} = 0.1 m_s$  is in progress. In these calculations the mass of the heavy quark is fixed at  $m_s$ , as determined from spectrum calculations with three equal mass quarks. In our spectrum runs at  $a = 0.13$  fm [6] we found that  $m_{\eta_{ss}}$  varied by less than 2% and  $m_\phi$  by less than 1% for  $0.2 m_s \leq m_{u,d} \leq m_s$  and the heavy quark mass held fixed at  $m_s$ . So, the neglect of the dependence of  $m_{\eta_{ss}}$  and  $m_\phi$  on  $m_{u,d}$  is well justified. In these studies, we performed linear interpolations of  $m_\pi^2$  and  $m_\rho$  at  $a = 0.20$  fm to determine the values of  $m_{u,d}$  for which  $m_\pi/m_\rho$  takes on the values found at  $a = 0.13$  fm. Then for  $0.13 \text{ fm} < a < 0.20 \text{ fm}$  we perform linear interpolations of the logarithms of  $a$ ,  $am_s$ , and  $am_{u,d}$  in the gauge coupling along lines of constant  $m_\pi/m_\rho$  and  $m_{\eta_{ss}}/m_\phi$ .

In all figures below we give the values of  $m_q/m_s$  for  $N_f = 3$  and  $m_{u,d}/m_s$  for  $N_f = 2 + 1$  at  $a = 0.13$  fm. The corresponding values of  $m_{\eta_{ss}}/m_\phi$  and  $m_\pi/m_\rho$  are given in Table 1.

For three equal mass quarks,  $N_f = 3$ , we have carried out thermodynamics studies on lattices with four, six and eight times slices, and aspect ratio  $N_s/N_t = 2$ . Here  $N_s$  and  $N_t$  are the spatial and temporal dimensions of the lattice in units of the lattice spacing. The spectrum calculations and interpolations described above allowed us to

Table 1

In the first column we show the value of  $m_q/m_s$  at lattice spacing 0.13 fm, which produced the  $m_{\eta_{ss}}/m_\phi$  ratio shown in the second column for spectrum calculations with three equal mass quarks. In the third column we give the value of  $m_{u,d}/m_s$  which produced the  $m_\pi/m_\rho$  ratio shown in the fourth column for spectrum calculations with two equal mass light quarks, and the mass of the heavy quark fixed at  $m_s$ .

$N_f = 3$		$N_f = 2 + 1$	
$m_q/m_s$	$m_{\eta_{ss}}/m_\phi$	$m_{u,d}/m_s$	$m_\pi/m_\rho$
1.0	0.673	1.0	0.673
0.6	0.583	0.6	0.582
0.4	0.504	0.4	0.509
		0.2	0.392

determine the values of the quark mass  $am_q$  that keep  $m_{\eta_{ss}}/m_\phi$  fixed as the gauge coupling is varied. They also enabled us to determine the value of the lattice spacing and, therefore, the temperature for each run.

In Fig. 1 we plot the real part of the Polyakov loop as a function of temperature on  $16^3 \times 8$  lattices. The Polyakov loop shows a crossover from confined behavior at low temperature to deconfined behavior at high temperature, but the transition is not particularly sharp. The insensitivity of the Polyakov loop to the quark mass at fixed temperature or lattice spacing is perhaps not surprising. We have determined the lattice spacing from the heavy quark potential, and in our spectrum runs we adjusted the coupling constant to keep the lattice spacing fixed as the quark mass is varied. Since the Polyakov loop, like the heavy quark potential, is determined from measurements of purely gluonic operators, our procedure is likely to minimize the dependence of the Polyakov loop on the quark mass.

In Fig. 2 we show the chiral order parameter,  $\bar{\psi}\psi$  as a function of temperature for  $m_q = m_s$ ,  $0.6 m_s$  and  $0.4 m_s$  on  $16^3 \times 8$  lattices. The black bursts in this figure are linear extrapolations of

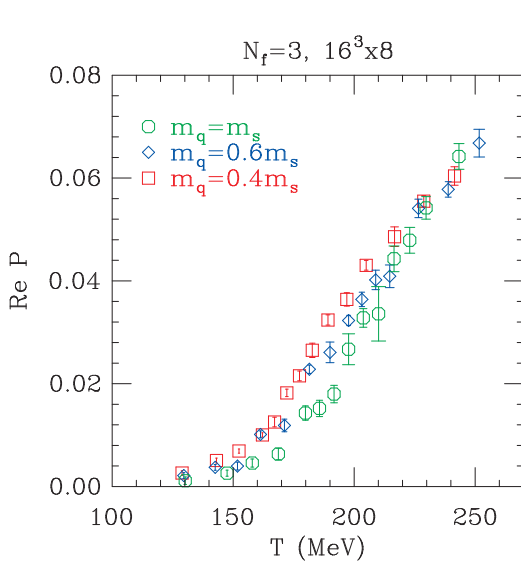


Figure 1. Real part of the Polyakov loop on  $16^3 \times 8$  lattices for three degenerate flavors of quarks.

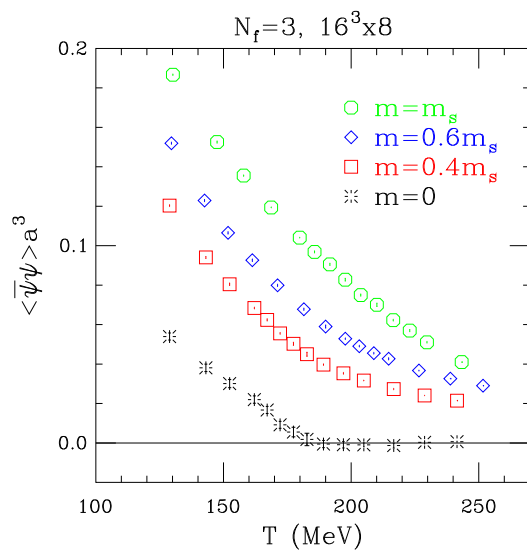


Figure 2. The chiral order parameter,  $\bar{\psi}\psi$ ,  $16^3 \times 8$  lattices. The black bursts are linear extrapolations in the quark mass to  $m_q = 0$  for fixed temperature.

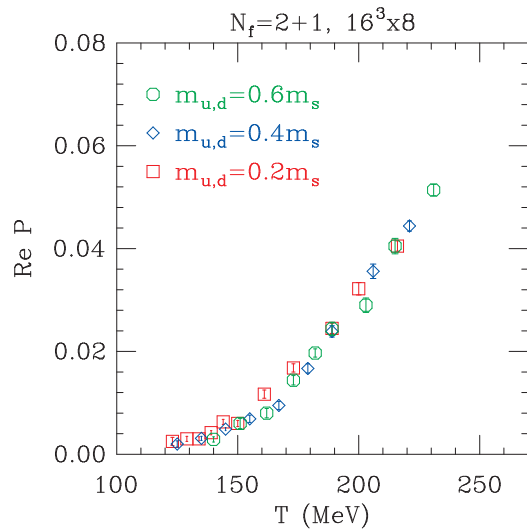


Figure 3. Real part of the Polyakov loop on  $16^3 \times 8$  lattices for two light and one heavy quark.

$\bar{\psi}\psi$  in the quark mass to  $m_q = 0$  for fixed temperature. All of these results are indicative of a crossover at the quark masses studied so far, rather than a *bona fide* phase transition. This result is consistent with earlier studies which found phase transitions only for smaller values of the quark mass than we have studied to date [7]. Fig. 2 suggests that there is unlikely to be a phase transition for temperatures above 180 MeV, but one could occur at or below that value.

The  $N_f = 2 + 1$  thermodynamics studies were carried out on  $12^3 \times 6$  and  $16^3 \times 8$  lattices. In this phase of our work we performed simulations with two degenerate light quarks and the heavy quark mass held equal to that of the strange quark. The spectrum calculations and interpolations described above allowed us to determine the values of the heavy and light quark masses needed to keep  $m_\pi/m_\rho$  and  $m_{\eta_{ss}}/m_\phi$  fixed as the gauge coupling was varied. They also allowed us to determine the lattice spacing, and therefore the temperature for each run.

In Fig. 3 we plot the real part of the Polyakov loop as a function of temperature on  $16^3 \times 8$  lattices for the three values of  $m_{u,d}$  studied to date. As in the  $N_f = 3$ , study we observe a crossover from confined to deconfined behavior, rather than

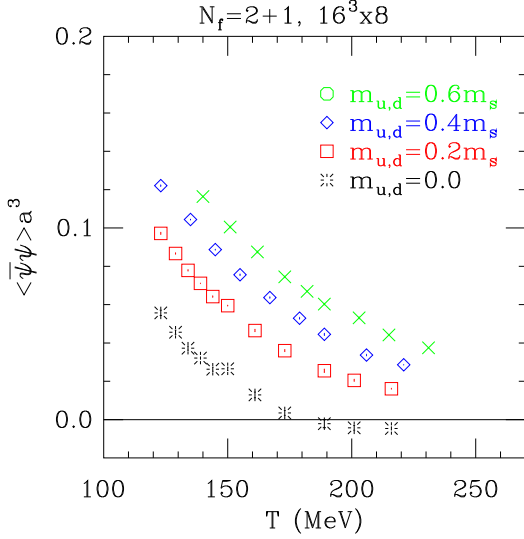


Figure 4. The chiral order parameter,  $\bar{\psi}\psi$ , on  $16^3 \times 8$  lattices. The black bursts are linear extrapolations in the quark mass to  $m_q = 0$  for fixed temperature.

a sharp transition, and little dependence on the light quark mass.

In Fig. 4 we plot the chiral order parameter as a function of temperature on  $16^3 \times 8$  lattices. The green, blue and red plotting symbols are data for  $m_{u,d} = 0.6 m_s$ ,  $0.4 m_s$  and  $0.2 m_s$  respectively, and the black bursts are linear extrapolations in  $m_{u,d}$  for fixed temperatures. As in the case of  $N_f = 3$ , all of these results are indicative of a crossover at the quark masses studied so far, rather than a *bona fide* phase transition. Fig. 4 suggests that for the heavy quark mass equal to that of the strange quark, there is unlikely to be a phase transition for  $T > 170$  MeV. Simulations at smaller values of  $m_{u,d}$  will be required to determine the precise location and the nature of the expected finite temperature transition. We plan to carry out such simulations during the coming year.

We have also measured quark number susceptibilities [8,9]. They can be related to event-by-event fluctuations in heavy ion collisions [10] by

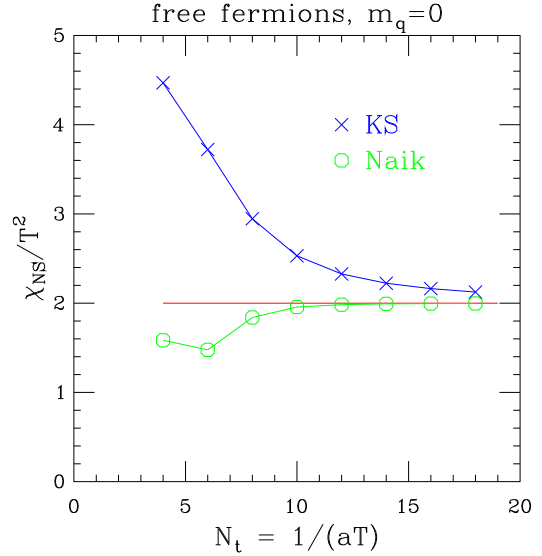


Figure 5. The quark number susceptibility for free Asqtad and standard staggered fermions as function of temporal lattice size  $N_t$ .

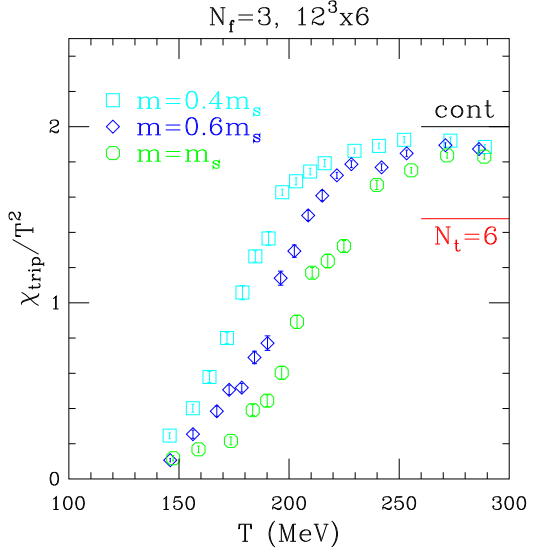


Figure 6. The triplet quark number susceptibility for  $N_f = 3$  on  $12^3 \times 6$  lattices. The black line on the right of the figure indicates the free quark value in the continuum, and the red line the free quark value on the finite lattices used.

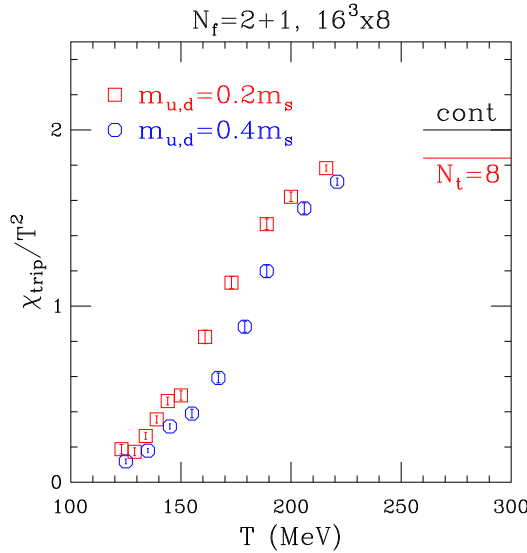


Figure 7. The triplet quark number susceptibility for  $N_f = 2 + 1$  on  $16^3 \times 8$  lattices. The black line on the right of the figure indicates the free quark value in the continuum, and the red line the free quark value on the finite lattices used.

the fluctuation-dissipation theorem

$$\langle \delta Q^2 \rangle \propto \frac{T}{V_s} \frac{\partial^2 \log Z}{\partial \mu_Q^2} = \chi_Q(T, \mu_Q = 0) , \quad (1)$$

with  $\mu_Q$  the chemical potential for the conserved charge  $Q$ , *e.g.* strangeness. We introduce a chemical potential  $\mu$  into the Asqtad action by

$$\begin{aligned} \mathcal{D}_{x,y}(\mu) &= \mathcal{D}^{spatial} + \\ \eta_0(x) &\left[ U_0^{(F)}(x) e^{\mu} \delta_{x+\hat{o},y} - U_0^{(F)\dagger}(x) e^{-\mu} \delta_{x,y+\hat{o}} \right. \\ &\left. + U_0^{(L)}(x) e^{3\mu} \delta_{x+3\hat{o},y} - U_0^{(L)\dagger}(x) e^{-3\mu} \delta_{x,y+3\hat{o}} \right] , \end{aligned} \quad (2)$$

where  $U_0^{(F)}$  is the time-like “fat-link” and  $U_0^{(L)}$  the time-like “long-link” including their tadpole improved coefficients.

Defining

$$\chi_{ij} = \left. \frac{T}{V_s} \frac{\partial^2 \log Z}{\partial \mu_i \partial \mu_j} \right|_{\mu=0} , \quad (3)$$

we computed the light-2-flavor singlet

$$\chi_{sing} = 2\chi_{uu} + 2\chi_{ud} \quad (4)$$

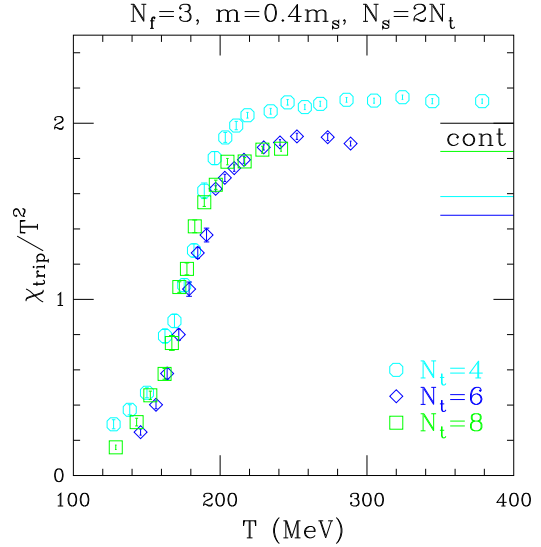


Figure 8. The triplet quark number susceptibility for  $N_f = 3$  with quarks of mass  $m_q = 0.4 m_s$ , on  $8^3 \times 4$ ,  $12^3 \times 6$  and  $16^3 \times 8$  lattices. The black line on the right of the figure indicates the value for free quarks in the continuum, and the colored lines the value for free quarks on the finite lattices used.

and triplet quark number susceptibility

$$\chi_{trip} = 2\chi_{uu} - 2\chi_{ud} , \quad (5)$$

using stochastic estimates with 100 random Gaussian sources. For  $N_f = 2 + 1$  we also computed the strange quark number susceptibility  $\chi_{strange} = \chi_{ss}$ .

For free fermions, the Asqtad action, because of the Naik term, reduces lattice artifacts significantly compared with the standard staggered action as demonstrated in Fig. 5.

In Figs. 6 and 7 we show the triplet susceptibility for the three quark masses we have studied in our  $N_f = 3$  simulations on  $12^3 \times 6$  lattices, and for the three values of  $m_{u,d}$  we have studied in our  $N_f = 2 + 1$  simulations on  $16^3 \times 8$  lattices, respectively. In Figs. 8 and 9 we show the triplet susceptibility for fixed quark mass for the different values of  $N_t$  used. In Fig. 9 we also show  $2 \times \chi_{ss}/T^2$ , a quantity which should become equal to  $\chi_{trip}/T^2$  in the very high temperature limit. We observe that the quark number susceptibil-

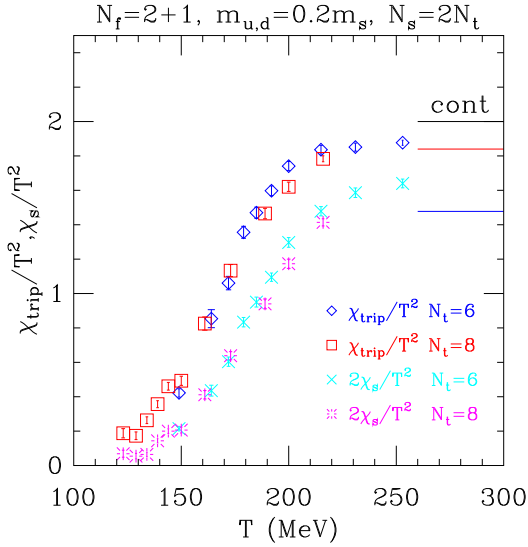


Figure 9. The triplet and strange quark number susceptibilities for  $N_f = 2+1$  with  $m_{u,d} = 0.2 m_s$  on  $12^3 \times 6$  and  $16^3 \times 8$  lattices. The black line on the right of the figure indicates the value for free quarks in the continuum, and the colored lines the value for free quarks on the finite lattices used.

ity provides a clean signal for the crossover from the hadronic to the quark-gluon plasma phase. The close agreement between the  $N_t = 6$  and 8 results in these figures is an indication of the excellent scaling properties in lattice spacing of the Asqtad action.

The singlet susceptibility looks very similar to the triplet susceptibility shown in Figs. 8 and 9. We show in Fig. 10 the difference between singlet and triplet susceptibility for  $N_f = 3$  at the lightest quark mass considered so far,  $m_q = 0.4 m_s$ . The two are clearly different in the crossover region.

This work is supported by the US National Science Foundation and Department of Energy and used computer resources at Florida State University (SP), NCSA, NERSC, NPACI, FNAL, and the University of Utah (CHPC).

## REFERENCES

1. Earlier reports on this work can be found in C. Bernard *et al.* (The MILC collaboration),

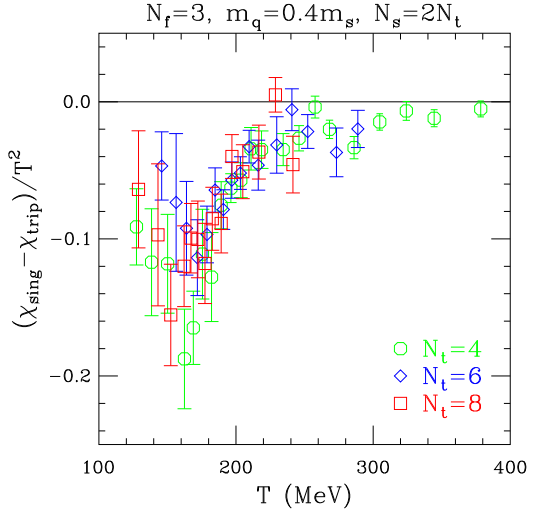


Figure 10. The difference between singlet and triplet quark number susceptibility for  $N_f = 3$  with quarks of mass  $m_q = 0.4 m_s$ , on  $8^3 \times 4$ ,  $12^3 \times 6$  and  $16^3 \times 8$  lattices.

2. K. Orginos, D. Toussaint and R.L. Sugar, Phys. Rev. D **60** (1999) 054503; Nucl. Phys. (Proc. Suppl.) **83** (2000) 878.
3. G.P. Lepage, Phys. Rev. D **59** (1999) 074501.
4. S. Naik, Nucl. Phys. **B316** (1989) 238.
5. C. Bernard *et al.* (The MILC collaboration), Phys. Rev. D **61** (2000) 111502.
6. C. Bernard *et al.* (The MILC collaboration), Phys. Rev. D **64** (2001) 054506.
7. S. Aoki *et al.* (JLQCD), Nucl. Phys. B (Proc. Suppl.) **73** (1999) 459; F. Karsch, E. Laermann and Ch. Schmidt, Phys. Lett. **B520** (2001) 41.
8. S. Gottlieb *et al.* Phys. Rev. Lett. **59** (1987) 2247.
9. R.V. Gavai and S. Gupta, Phys. Rev. D **64** (2001) 074506; Phys. Rev. D **65**, (2002) 094515; R.V. Gavai, S. Gupta and P. Majumdar, Phys. Rev. D **65** (2002) 054506.
10. B. Müller, Nucl. Phys. A **702** (2002) 281; V. Koch, M. Bleicher and S. Jeon, Nucl. Phys. A **702** (2002) 291; R.V. Gavai, Nucl. Phys. A **702** (2002) 299.